ARTICLE

THE ANALYST
www.rsc.org/analyst

Mediated amperometric immunosensing using single walled carbon nanotube forests†‡

Máire O'Connor,[a] Sang Nyon Kim,[b] Anthony J. Killard,[a] Robert J. Forster,[a] Malcolm R. Smyth,[a] Fotios Papadimitrakopoulos[b] and James F. Rusling[c]

[a] *National Centre for Sensor Research, Dublin City University, Dublin 9, Ireland*

[b] *Nanomaterials Optoelectronics Laboratory, Polymer Program, Institute of Materials Science, University of Connecticut, Storrs, CT 06269, USA*

[c] *Department of Chemistry, University of Connecticut, U-60, 55 North Eagleville Road, Storrs, CT06269-3060, Department of Pharmacology, University of Connecticut Health Center, Farmington, CT 06032, USA*

Received 19th August 2004, Accepted 15th October 2004
First published as an Advance Article on the web 12th November 2004

A prototype amperometric immunosensor was evaluated based on the adsorption of antibodies onto perpendicularly oriented assemblies of single wall carbon nanotubes called SWNT forests. The forests were self-assembled from oxidatively shortened SWNTs onto Nafion/iron oxide coated pyrolytic graphite electrodes. The nanotube forests were characterized using atomic force microscopy and resonance Raman spectroscopy. Anti-biotin antibody strongly adsorbed to the SWNT forests. In the presence of a soluble mediator, the detection limit for horseradish peroxidase (HRP) labeled biotin was 2.5 pmol ml^{-1} (2.5 nM). Unlabelled biotin was detected in a competitive approach with a detection limit of 16 nmol ml^{-1} (16 μM) and a relative standard deviation of 12%. The immunosensor showed low non-specific adsorption of biotin–HRP (approx. 0.1%) when blocked with bovine serum albumin. This immunosensing approach using high surface area, patternable, conductive SWNT assemblies may eventually prove useful for nano-biosensing arrays.

Introduction

Since their discovery,[1–3] carbon nanotubes (CNTs) have attracted increasing attention due to their unique structural,[4] mechanical[5] and electronic[6] properties. Practical applications have been found in many fields. Recently there have been several reports on their application in the area of electrochemical biosensing.[7–17] Their nanometer dimensions, combined with high electrical conductivity, may promote electron transfer to and from redox proteins including cytochrome c,[7] horseradish peroxidase (HRP),[8] myoglobin, and glucose oxidase.[9] This has allowed the sensitive detection of glucose, hydrogen peroxide and nitric oxide.[10] Improved electrochemical behaviour of catecholamine neurotransmitters[11] and NADH[12] has been demonstrated. CNTs have also provided sensitive DNA hybridization detection.[13,14] Advances in the fabrication of biomaterial-CNT hybrid systems and their potential application in different nanobioelectronic systems has recently been extensively reviewed.[15]

A few reports have been published concerning the application of CNT in the field of immunosensing. Chen *et al.* (2003) developed sensitive CNT-based immunoassays making use of two different transduction mechanisms. In the first a single walled nanotube (SWNT) film was formed on a quartz crystal surface and mass changes were measured using a quartz crystal microbalance. The second involved a transistor configuration featuring a layer of interconnected SWNT bridging two Ti/Au electrodes.[16] The antigen, a U1A RNA splicing factor, was conjugated to Tween 20 which adsorbed to the SWNTs. Detection of an autoantibody specific for this factor was achieved by both systems at concentrations $\leqslant$1 nM. However, with regards to the transistor configuration, subsequent work showed that proteins adsorbed to metal–nanotube junctions of similar devices causing the observed resistance changes, and proteins which adsorbed only to the carbon nanotubes gave no change in resistance.[17] A CNT–poly(ethylene vinylacetate) EVA composite was used to develop an immunoassay that detected electrochemiluminescence (ECL).[18] Disks of the nanotube composite were acid oxidized. Subsequently strepavidin was covalently bound and biotinylated anti-α-fetoprotein (AFP) immobilized. The introduction of AFP and an anti-AFP monoclonal antibody labeled with $[Ru(bpy)_3]^{2+}$ resulted in the formation of a sandwich complex. The ECL signal obtained using a sacrificial reductant provided a limit of detection of 0.1 nM of AFP.

The patternable, conductive, nanoscale structures of SWNT forest provides new opportunities in the development of nano-immunosensor arrays. This report constitutes an introductory investigation into the feasibility of amperometric immunosensing based on the SWNT forest assembly reported previously.[19] The technique is based on the coordination of the carboxylic acid groups of acid oxidized SWNT to Fe^{3+} adsorbed on a Nafion-coated pyrolytic graphite electrode. Previously, when SWNTs were assembled on pyrolytic graphite using this method and immobilized HRP or myoglobulin a limit of detection of H_2O_2 of 70 nM and 50 nM, respectively, was obtained by our group.[8] Other groups have also reported the use of metal-assisted assembly to align SWNT normal to substrates involving Zn,[20] Ag[21] and Cu.[22]

Various methods have been used to attach biomolecules onto CNTs. These include hydrophobic[23] or electrostatic interactions with the side walls or by functionalization of the nanotube sides by hydrophobic molecules, *i.e.*, 1-pyrenebutanoic

† Presented at the Symposium on "Nanotechnology: Surfaces, Sensors and Systems" at the 10th International Conference on Electroanalysis, June 6–10, 2004, Galway, Ireland.

‡ Electronic supplementary information (ESI) available: section analyses of AFM images on smooth silicon of Nafion/Fe_2O_3 and Nafion/Fe_2O_3/SWNT. See http://www.rsc.org/suppdata/an/b4/b412805b/

DOI: 10.1039/b412805b

acid succinimidyl ester[24] or bioconjugates of Tween 20.[16] It is important to functionalise the side walls in noncovalent ways to preserve the sp^2 nanotube structure and electronic characteristics. Attachment *via* covalent bonding with COOH functional groups also provides a convenient method and has been successfully applied in the covalent binding of redox proteins such as glucose oxidase,[25] myoglobin, HRP[8] and peptide nucleic acids.[26] In an alternative approach, we covalently bound antibodies to SWNT forests and detected antigen–antibody binding by direct catalytic reduction of hydrogen peroxide by horseradish peroxidase labels.[27] In this report, the simpler approach of strong adsorption between the antibody and the SWNT surface was used with a soluble mediator to couple the majority of the enzyme label reaction to the measuring circuit. Results suggest the feasibility of using SWNT forests for sensitive mediated amperometric immunodetection.

Experimental

Reagents

SWNT (HiPCO) were purchased from Tubes@rice (90% pure). All other chemicals were reagent grade and purchased from Sigma–Aldrich. Anti-biotin antibody was a goat polyclonal (B-3640) and horseradish peroxidase-labeled biotin (biotin-HRP) was biotinamidocaproyl-labeled peroxidase (P-9568).

Instrumentation

Electrochemical measurements. Cyclic voltammetry and amperometry were performed with a CHI 660 potentiostat. A three electrode cell was used employing a saturated calomel reference electrode, a platinum wire as counter electrode and ordinary plane pyrolytic graphite as working electrode. (Advanced Ceramics, area of 0.2 cm^2). The electrochemical buffer was pH 6.8 phosphate buffer, 0.1 M, 0.137 M NaCl and 2.7 mM KCl. The buffers were purged with purified nitrogen and a nitrogen environment was maintained in the cell during experiments.

Atomic force microscopy. Tapping mode measurements were performed on smooth Si(100) wafers with a Nanoscope IV scanning probe microscope.

Resonance Raman measurements. Resonance Raman spectra of SWNT forest assemblies on pyrolytic graphite electrodes were taken with a Renishaw Ramanscope 2000 using a 785 nm (1.58 eV) argon laser focused on a 1 μm spot by a 100× objective lens.

Methods

Assembly of SWNT forests

SWNT forests were constructed on basal plane pyrolytic graphite disk electrodes that were first abraded on 400 grit SiC paper, then ultra-sonicated in water for 1 min. The SWNTs were carboxyl functionalized and shortened by sonication in a mixture of HNO_3 and H_2SO_4 for 4 hours at 70 °C. The electrodes were dipped in 1 mg ml^{-1} Nafion solution in 9 : 1 (v/v) methanol–water for 15 min. This was quickly washed with water and then placed in 5 mg ml^{-1} of $FeCl_3 \cdot 6H_2O$ for 15 min. After washing with water the electrodes were then placed in a freshly sonicated DMF suspension of SWNTs for 30 min, washed with methanol and dried.

Immunoassay procedure

Anti-biotin antibody was prepared unless otherwise stated at 0.5 mg ml^{-1} in pH 7.2, 0.01 M phosphate buffer, 0.137 M NaCl, 2.7 mM KCl (PBS) and allowed to incubate on an SWNT surface for 3 hours. Excess antibody was removed by washing with PBS containing 0.05% Tween 20, followed by washing with PBS. This washing step was repeated after each incubation. The surface was then blocked with 2% bovine serum albumin (BSA) in PBS. The competition step involved incubating biotin (dissolved in PBS) and biotin-HRP simultaneously on the antibody immobilized and BSA blocked SWNT surface for 1 hour.

Electroanalytical procedure

Rotating disk amperometry was performed at −0.3 V *versus* SCE at 2000 rpm with 1 mM hydroquinone and 400 μM H_2O_2 unless otherwise stated.

Results

Characterization studies

Atomic force microscopy (AFM) images were taken on smooth silicon wafers at each step of the assembly, *i.e.*, after deposition of Nafion, Fe_2O_3 and SWNT layers and also after antibody adsorption (Fig. 1 and electronic supplementary information

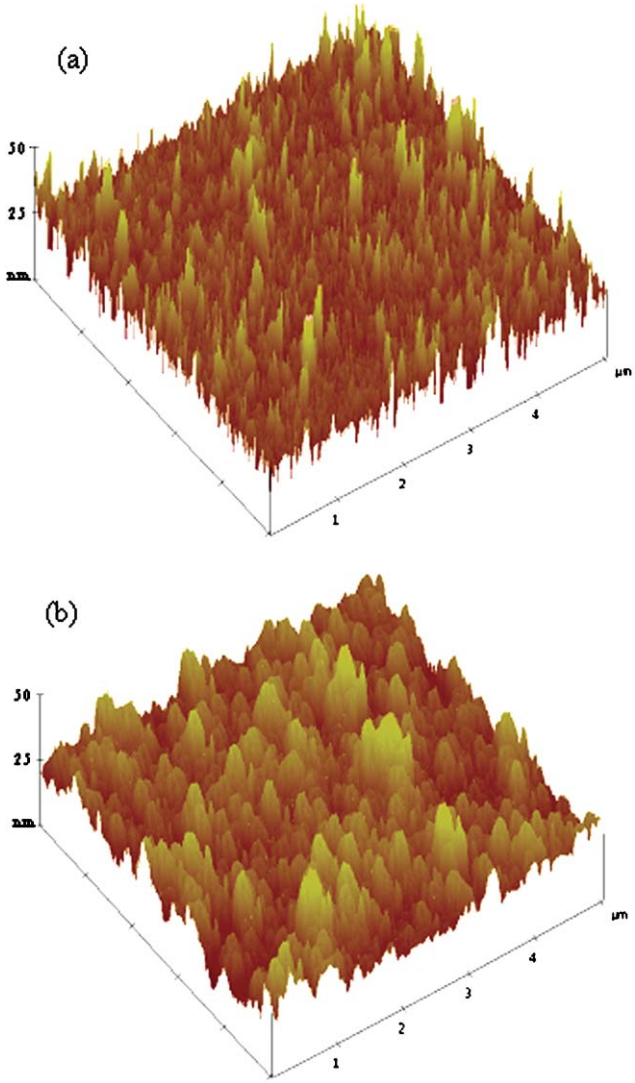

Fig. 1 Tapping mode AFM image of (a) Nafion/Fe_2O_3/SWNT (b) Nafion/Fe_2O_3/SWNT/antibody. The SWNT image showed a densely packed assembly with a protrusion height of 26 ± 6 nm. Adsorption of antibody resulted in a large increase in domain width of 187 ± 44 nm and a more aggregated globular appearance.

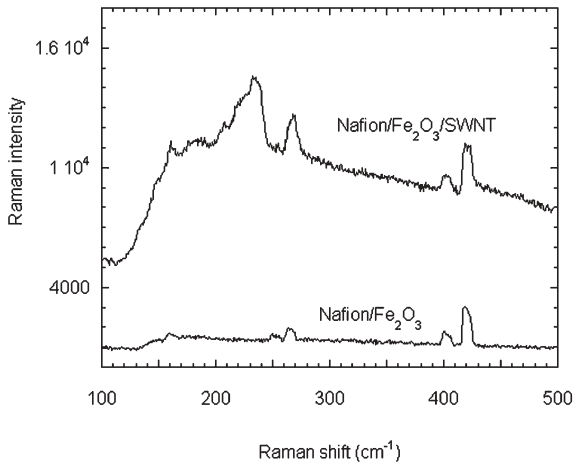

Fig. 2 Resonance Raman spectra (1.58 eV) of Nafion/iron oxide/SWNT and Nafion/iron oxide on pyrolytic graphite.

Fig. S1‡). Section analysis of the Nafion layer showed peak heights between 1–2 nm. A large contrast to this can be seen on addition of the Fe_2O_3 layer. The peak height from section analysis of Nafion/Fe_2O_3 layer displayed a height of 29 $\pm$ 10 nm. The domain width of the iron islands was 209 $\pm$ 32 nm. After assembly of SWNT the section analysis resulted in a far more densely packed layer with protrusion height of 26 $\pm$ 6 nm. The top view showed a dense granular appearance of the SWNT with dimensions of 96 $\pm$ 25 $\times$ 30 $\pm$ 10 nm. Although there are contributions to these measurements from the AFM tip broadening effect, this may also suggest the formation of SWNT bundles due to hydrophobic forces. Adsorption of antibody resulted in an AFM image with a more aggregated appearance. The domain width of these aggregates was found to be 187 $\pm$ 44 nm.

Resonance Raman spectroscopy was also used to confirm the assembly of SWNT on pyrolytic graphite electrodes. Fig. 2 shows that a peak at 230 cm^{-1}, which is characteristic of radial breathing mode of SWNT, is present in the spectra of the Nafion/Fe_2O_3/SWNT assembly. This peak is absent in the spectra of Nafion/Fe_2O_3 and that from the bare pyrolytic graphite electrode. This confirms successful assembly of SWNT forests on pyrolytic graphite.

Optimization of immunosensor variables

Variables such as concentration of adsorbed antibody, biotin–HRP, hydroquinone and hydrogen peroxide were optimized. Saturation of the surface was found with 0.5 mg ml^{-1} antibody. In the case of biotin–HRP the current showed a linear increase with increasing concentration until 25 pmol ml^{-1} (1 μg ml^{-1}) was reached (Fig. 3). The high currents obtained are the result of the oxidation of HRP by H_2O_2 and the catalytic reduction back to its original form by hydroquinone.

At concentrations greater than 75 pmol ml^{-1} (3 μg ml^{-1}) of biotin–HRP a decrease in current was observed. This suggests that the diffusion of hydroquinone may be impeded by steric hindrance from the increasing concentration of biotin–HRP. This is a characteristic of diffusion controlled mediators whereby their redox reaction may be suppressed due to a decrease in the electrode active area and/or an increase in the distance that marker ions can approach the electrode active surface.[28] The optimum concentration of biotin–HRP for use in the competition assay was therefore chosen as 25 pmol ml^{-1}. While optimal concentrations of reagents have been determined here, additional information could be derived to establish the mass of antibody and conjugate immobilized. This could be achieved, for example, by using either

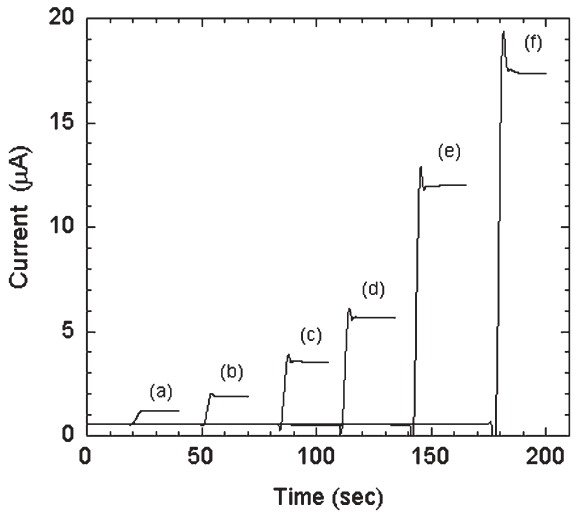

Fig. 3 Amperograms showing effect of concentration of biotin–HRP on catalytic current. These were obtained at 2000 rpm, 300 μM hydroquinone and 150 μM H_2O_2 at −0.3 V. The concentrations of Biotin–HRP were (a) 1 (b) 3 (c) 5 (d) 10 (e) 15 (f) 25 pmol ml^{-1}.

fluorescently labeled reagents or a colorimetric assay of the HRP labeled components.

The non-specific adsorption of biotin-HRP was assessed. This was determined by incubating a mouse anti-IgG on the surface, blocking with 2% BSA in the usual way and measuring the current after incubation with biotin–HRP. Since this antibody is not specific for biotin–HRP any catalytic current generated in this case is indicative of non-specific adsorption of biotin–HRP on the surface. Very low current was observed showing that at a biotin–HRP concentration of 25 pmol ml^{-1} only 0.1% of the current was due to non-specific adsorption of biotin-HRP.

In the case of hydroquinone concentration the catalytic current undergoes large increases with addition of 100 μM hydroquinone and levels off at 1 mM where saturation is reached. 1 mM was therefore chosen for use in the competitive assay (Fig. 4a).

The effect of the concentration of H_2O_2 on the amperometric current was monitored (Fig. 4b). On addition of H_2O_2 the current increased at approximately 0.08 μA μM^{-1} H_2O_2 for concentrations of H_2O_2 between 200 μM and 1 mM. The rsd also increased with each successive addition of H_2O_2. With the addition of 200 μM H_2O_2 the rsd was 11.9% but this had increased to an rsd of 13.6% when the concentration of H_2O_2 had reached 1 mM. A concentration of 400 μM was chosen for the competition assay as a compromise between obtaining a high signal and better reproducibility.

The semilogarithmic graph of current *versus* biotin concentration shown in Fig. 5 showed that the response decreased with less enzyme conjugate binding to the immobilized antibody, as the concentration of free biotin in solution increased. A linear range can be seen within the biotin concentrations of 4 nmol ml^{-1} and 120 nmol ml^{-1}.

The SWNT forest electrodes with all the immunoassay components immobilized could be stored in a humid aerobic chamber at 4 °C for one week with no significant change to the amperometric current. The current obtained under these conditions was 16.7 $\pm$ 1.6 μA, whereas the current obtained when the amperometry was preformed immediately was 17.3 $\pm$ 2.2 μA (n = 5). However, after the electrodes were stored for one week in PBS buffer the average amperometric current generated was 9.9 $\pm$ 1.3 μA (n = 4, rsd = 13.4%). This represents a decrease of 43% from the original signal.

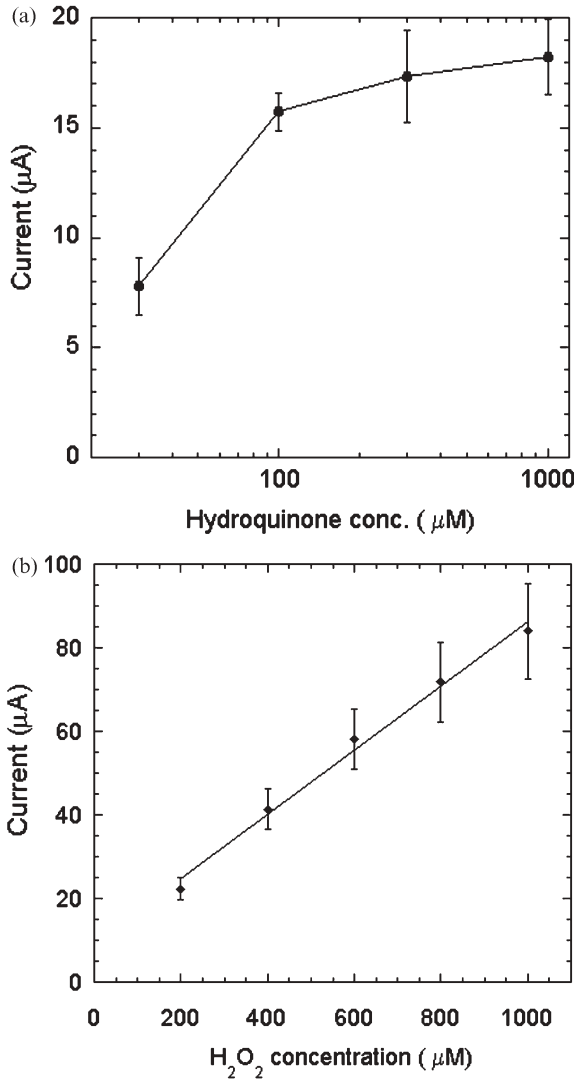

Fig. 4 (a) Effect of hydroquinone concentration on amperometric steady state current with 150 μM H_2O_2. (b) Current *versus* H_2O_2 concentration with 1 mM hydroquinone. Both at −0.3 V, 0.5 mg ml^{-1} antibody, 25 picomol ml^{-1} biotin–HRP, 2000 rpm, $n = 3$.

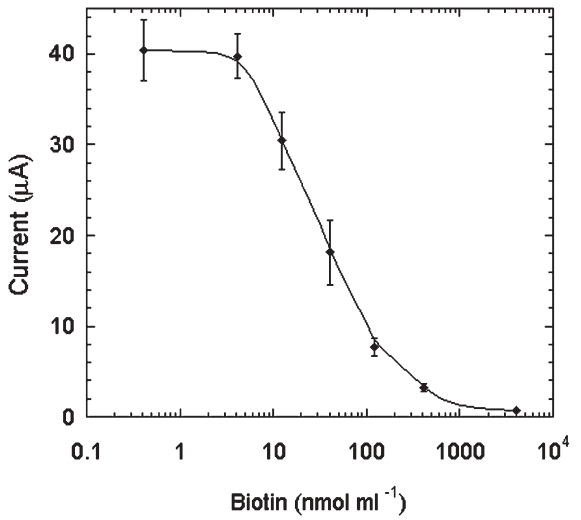

Fig. 5 Influence of biotin concentration on steady state amperometric current with 25 pmol ml^{-1} biotin–HRP, 400 μM H_2O_2 and 1 mM hydroquinone, 2000 rpm, $n = 3$.

Discussion

Results show that the SWNT forests with a strongly adsorbed antibody are suitable for use as high-sensitivity amperometric immunosensors. In the presence of a soluble mediator, the detection limit for horseradish peroxidase labeled biotin was 2.5 pmol mL^{-1} (0.1 μg ml^{-1}). This corresponds to the limit of detection expected from a traditional ELISA experiment.[29] Unlabelled biotin was detected in a competitive assay with a detection limit of 16 nmol ml^{-1} (16 μM) and relative standard deviation of 12%. Compared to a related method where anti-biotin was covalently linked to SWNT forests and direct, unmediated amperometric detection of the enzyme label used,[27] the detection limits of the present mediated system are about 10-fold better, probably because nearly all of the enzyme label is linked to the measurement by the mediation.

Control experiments showed that there was low non-specific adsorption of biotin–HRP. BSA effectively blocked most free sites on the SWNT surface. No significant change in current was observed when the electrodes were stored in a humid chamber at 4 °C for one week. The disadvantage of the antibody adsorption approach is that while the storage stability is good, the stability in buffer was poor. This suggests that the immunosensors in this work are usable only for several days. However, simplicity of sensor construction is also an advantage.

In these experiments hydroquinone was used as a mediator. Mediators are small, redox active molecules with inherently high heterogeneous electron transfer rates and are frequently used to increase the heterogeneous electron transfer of peroxidases. Mediators are especially useful when the peroxidase is at a distance from the electrode surface as in the case of immunoassays. Hydroquinone is one of the most efficient electron donors to HRP with a reaction rate as high as 1.2×10^7 M^{-1} s^{-1}.[30] However, future SWNT immunosensor configurations are being pursued in which polymeric mediators or conductive polymers are incorporated to replace the soluble mediator to achieve a reagentless sensor. HRP is known to show a decreasing activity when H_2O_2 is present with the degree of inactivation being dependent on the incubation time and the hydrogen peroxide concentration.[31]

The SWNT assembly process used here and developed previously involves the self-assembly of oxidatively shortened SWNT onto Fe^{3+}–Nafion underlayers.[19] The electrodes were coated with Nafion to achieve a uniform negatively charged surface suitable for a high surface coverage of Fe_2O_3. The layer of Fe_2O_3 was formed by immersion of the electrode in an aqueous solution of $FeCl_3$. Several factors may come into play to produce a successful assembly of SWNT. The driving force for the assembly may be due to acid/base neutralization between iron hydroxides and the carboxylic acid groups of the SWNT.[19] Since carboxylic acids can be deprotonated by various metal oxides the SWNT assembly process may also be promoted by coulombic forces between the carboxylate anion headgroup and iron oxides coated on the substrate. This mechanism has been proposed for the assembly of carboxylic acid functionalised SWNT on zinc[20] and silver[21] oxide surfaces.

The assembly was characterised by both AFM and resonance Raman spectroscopy. A distinct change in the AFM image was seen after deposition of each layer of the assembly (Fig. 1). A densely packed and uniform surface coverage of the SWNT was found. The protrusion height of the SWNT obtained here (26 ± 6 nm) is in agreement with other reports in the literature, where acid oxidised SWNT are assembled on various metals.[19–21] A uniform surface coverage of anti-biotin antibody was also observed.

Resonance Raman spectroscopy is also an effective tool for the characterization of SWNT assemblies. SWNTs have 15 or

16 Raman active vibrational modes. The exact number depends on the symmetry of the tube but is independent of the diameter.[32] Four of the Raman bands are strongly resonance-enhanced. Three of these are located around 1600 cm^{-1} and correspond to the characteristic A, E_1 and E_2 modes of the graphene sheet. The fourth band, at around 200 cm^{-1}, is caused by the radial breathing mode (RBM), where all atoms move in phase perpendicular to the tube axis, changing the radius of the tube. The radial frequency is sensitive to the diameter only and not to the helicity of the nanotube. Since the RBM is unique to nanotubes without any counterpart in graphite it can be used to confirm the assembly of SWNT on pyrolytic graphite electrodes. Fig. 2 shows that a peak at 230 cm^{-1} is present in the 1.58 eV resonance Raman spectra of the SWNT assembly. This is characteristic of the radial breathing mode of SWNTs and is not present in the spectra of either the bare pyrolytic graphite electrode or pyrolytic graphite/Nafion/Fe_2O_3 control. Controls have been performed where the antibody was linked to Nafion/Fe_2O_3 coated electrodes. As expected, a large current was obtained after reaction with biotin-HRP, showing that the CNTs are in good electronic communication with the electrode.

Conclusions

Results herein demonstrate that SWNT forest electrodes can be used to develop a sensitive amperometric immunosensor. Antibodies were adsorbed on the surface of the SWNTs to give competitive assay results for biotin with an average rsd of ~12%. The limit of detection of biotin–HRP was 2.5 pmol ml^{-1} (2.5 nM) and that of biotin was 16 nmol ml^{-1} (16 μM). The surfaces of the nanotubes were effectively blocked with BSA to result in low non-specific binding of biotin–HRP. While the limits of detection achieved here might be further improved, for example by using high affinity monoclonal antibodies, the feasibility of high sensitivity mediated immunosensing on SWNT forest platforms has been demonstrated.

Acknowledgements

This work was supported by U.S. Army Research Office (ARO) *via* grant DAAD-02-1-0381.

References

1 S. Iijima, *Nature.*, 1991, **354**, 56.
2 S. Iijima and T. Ichihashi, *Nature*, 1993, **363**, 603.
3 D. S. Bethune, C. H. Kiang, M. S. de Vries, G. Gorman, R. Savoy, J. Vazquez and R. Beyers, *Nature*, 1993, **363**, 605.
4 P. M. Ajayan, *Chem. Rev.*, 1999, **99**, 1787.
5 J. P. Salvetat-Delmotte and A. Rubio, *Carbon*, 2002, **40**, 1729.
6 D. T. Colbert and R. E. Smalley, *TIBTECH*, 1999, **17**, 46.
7 J. Wang, M. Li, Z. Shi, N. Li and Z. Gu, *Anal. Chem.*, 2002, **74**, 1993.
8 X. Yu, D. Chattopadhyay, I. Galeska, F. Papadimitrakopoulos and J. F. Rusling, *Electrochem. Commun.*, 2003, **5**, 408.
9 S. G. Wang, Q. Zhang, R. Wang, S. F. Yoon, J. Ahn, D. J. Yang, J. Z. Tian, J. Q. Li and Q. Zhou, *Electrochem. Commum.*, 2003, **5**, 800.
10 G. C. Zhao, L. Zhang, X. W. Wei and Z. S. Yang, *Electrochem. Commun.*, 2003, **5**, 825.
11 Z. Wang, J. Liu, Q. Liang, Y. Wang and G. Luo, *Analyst*, 2002, **127**, 653.
12 M. Musameh, J. Wang, A. Merkoci and Y. Lin, *Electrochem. Commun.*, 2002, **4**, 743.
13 J. Wang, G. Liu, M. Rasul Jan and Q. Zhu, *Electrochem. Commun.*, 2003, **5**, 1000.
14 J. Wang, A. N. Kawde and M. Musameh, *Analyst*, 2003, **128**, 912.
15 E. Katz and I. Willner, *Chem. Phys. Chem.*, 2004, **5**, 1084.
16 R. J. Chen, S. Bangsaruntip, K. A. Drouvalakis, N. Wong shi Kam, M. Shim, Y. Li, W. Kim, P. J. Utz and H. Dai, *Proc. Am. Chem. Soc.*, 2003, **100**, 4984.
17 R. J. Chen, H. C. Choi, S. Bangsaruntip, E. Yenilmez, X. Tang, Q. Wang, Y.-L. Chang and H. Dai, *J. Am. Chem. Soc.*, 2004, **126**, 1563.
18 J. N. Wohlstadter, J. L. Wilbur, G. B. Sigal, H. A. Biebuyck, M. A. Billadeau, L. Dong, A. B. Fischer, R. Satyanarayana, S. H. Gudibande, J. H. Jamieson, J. L. Kenton, J. K. Leland, R. J. Massey and S. J. Wohlstadter, *Adv. Mater.*, 2003, **15**, 1184.
19 D. Chattopadhyay, I. Galeska and F. Papadimitrakopoulos, *J. Am. Chem. Soc.*, 2001, **123**, 9451.
20 X. Yu, T. Mu, H. Huang, Z. Liu and N. Wu, *Surface Sci.*, 2000, **461**, 199.
21 B. Wu, J. Zhang, W. Zhong, C. Shengmin and Z. Liu, *J. Phys. Chem. B.*, 2001, **105**, 5075.
22 L. Cai, J. L. Bahr, Y. Yao and J. M. Tour, *Chem. Mater.*, 2002, **14**, 4235.
23 F. Balavoine, P. Schultz, C. Richard, V. Mallouh, T. W. Ebbesen and C. Mioskowski, *Angew. Chem. Int. Ed.*, 1999, **38**, 1912.
24 R. J. Chen, Y. Zhang, D. Wang and H. Dai, *J. Am. Chem. Soc.*, 2001, **123**, 3838.
25 H. Xue, W. Sun, B. He and Z. Shen, *Synth. Met.*, 2003, **135–136**, 833.
26 K. A. Williams, T. M. Veenhuizen, B. G. de la Torre, R. Eritja and C. Dekker, *Nature*, 2002, **420**, 761.
27 X. Yu, S. N. Kim, F. Papadimitrakopoulos and J. F. Rusling, *J. Am. Chem. Soc.*, submitted for publication.
28 H. Kuramitz, M. Matsuda, J. H. Thomas, K. Sugawara and S. Tanaka, *Analyst*, 2003, **128**, 182.
29 B. Lu, E. I. Iwuoha, M. R. Smyth and R. O'Kennedy, *Anal. Chim. Acta*, 1997, **345**, 59.
30 T. Ruzgas, E. Csoregi, J. Emneus, L. Gorton and G. Marko-Varga, *Anal. Chim. Acta*, 1996, **330**, 123.
31 A. Schmidt, J. T. Schumacher, J. Reichelt, H. J. Hecht and U. Bilitewski, *Anal. Chem.*, 2002, **74**, 3037.
32 J. Kurti, G. Kresse and H. Kurzmany, *Phys. Rev. B*, 1998, **58**, R8869.